HHS Public Access

Author manuscript

Toxicol Appl Pharmacol. Author manuscript; available in PMC 2017 January 15.

Published in final edited form as:

Toxicol Appl Pharmacol. 2016 January 15; 291: 21–27. doi:10.1016/j.taap.2015.12.003.

Irinotecan (CPT-11)-induced elevation of bile acids potentiates suppression of IL-10 expression

Zhong-Ze Fang[1,2,3], **Dunfang Zhang**[4], **Yun-Feng Cao**[3], **Cen Xie**[1], **Dan Lu**[5], **Dong-Xue Sun**[1], **Naoki Tanaka**[1], **Changtao Jiang**[1], **Qianming Chen**[4], **Yu Chen**[4], **Haina Wang**[6], and **Frank J. Gonzalez**[1,*]

[1]Laboratory of Metabolism, Center for Cancer Research, National Cancer Institute, National Institutes of Health, Bethesda, Maryland, USA

[2]Department of Toxicology, School of Public Health, Tianjin Medical University, Tianjin, China

[3]Joint Center for Translational Medicine, Dalian Institute of Chemical Physics, Chinese Academy of Sciences and First Affiliated Hospital of Liaoning Medical University, Dalian, China

[4]State Key Laboratory of Oral Diseases, West China Hospital of Stomatology, Sichuan University, Chengdu, China

[5]Department of Immunology, Tianjin Key Laboratory of Cellular and Molecular Immunology, Tianjin Medical University, Tianjin, China

[6]School of Pharmaceutical Sciences, Shandong University, Jinan, China

Abstract

Irinotecan (CPT-11) is a first-line anti-colon cancer drug, however; CPT-11-induced toxicity remains a key factor limiting its clinical application. To search for clues to the mechanism of CPT-11-induced toxicity, metabolomics was applied using ultra-performance liquid chromatography coupled with electrospray ionization quadrupole time-of-flight mass spectrometry. Intraperitoneal injection of 50 mg/kg of CPT-11 induced loss of body weight, and intestine toxicity. Changes in gallbladder morphology suggested alterations in bile acid metabolism, as revealed at the molecular level by analysis of the liver, bile, and ileum metabolomes between the vehicle-treated control group and the CPT-11-treated group. Analysis of immune cell populations further showed that CPT-11 treatment significantly decreased the IL-10-producing CD4 T cell frequency in intestinal lamina propria lymphocytes, but not in spleen or mesenteric lymph nodes. *In vitro* cell culture studies showed that the addition of bile acids deoxycholic acid and taurodeoxycholic acid accelerated the CPT-11-induced suppression of IL-10 secretion by activated $CD4^+$ naive T cells isolated from mouse splenocytes. These results showed

*Corresponding author: Frank J. Gonzalez, Laboratory of Metabolism, Center for Cancer Research, National Cancer Institute, National Institutes of Health, Bethesda, MD, 20892. gonzalef@mail.nih.gov.

Conflicts of Interest

There are no conflicts of interest to report.

that CPT-11 treatment caused metabolic changes in the composition of bile acids that altered CPT-11-induced suppression of IL-10 expression.

Graphical Abstract

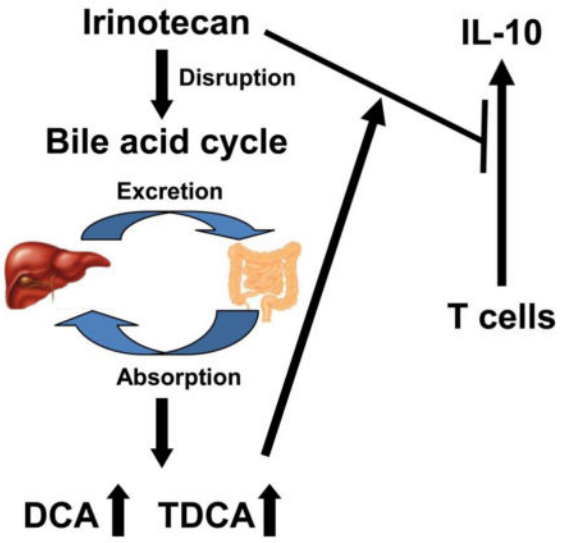

Keywords

irinotecan (CPT-11); metabolomics; bile acids; interleukin-10

Introduction

Irinotecan, also called CPT-11, is a topoisomerase 1 inhibitor used for the treatment of colon cancer (Nygard *et al.*, 2014). However, CPT-11 treatment leads to adverse effects, including leukopenia (Umezawa *et al.*, 2000), diarrhea (Xue *et al.*, 2007), and mucositis (Lima-Junior *et al.*, 2014). The mechanisms for these toxic responses were investigated, revealing a significant contribution of the intestinal drug-metabolizing enzyme UDP-glucuronosyltransferase (UGT) 1A1 towards CPT-11-induced intestinal damage (Iyer *et al.*, 1998; Chen *et al.*, 2013). Interleukin-33 (IL-33) was also demonstrated to mediate CPT-11-induced intestinal mucositis and severe diarrhea, and inhibition of the IL-33/ST2 pathway could limit mucositis (Guabiraba *et al.*, 2014). Targeted inhibition of interleukin-18 (IL-18) can attenuate CPT-11-induced intestinal mucositis in mice (Lima-Junior *et al.*, 2014). However, the mechanism by which these cytokines are altered remains to be defined.

Metabolomics is an important tool in determining the compositions and levels of metabolites in a serum, urine, cells, and tissues,. Through analyzing the biological function of altered metabolites, clues to the mechanisms of toxicity can sometimes identified. For example, an important role of lipid metabolism in trichloroethylene-induced liver toxicity was revealed using metabolomics (Fang *et al.*, 2013). Gemfibrozil-induced disruption of lysophosphatidylcholine and bile acid homeostasis was found to be a key factor in gemfibrozil-induced hepatotoxicity (Liu *et al.*, 2014). The present study aimed to investigate

the mechanism of CPT-11-induced metabolic disorders by analysis of endogenous metabolites using metabolomics. Furthermore, the function of metabolites altered by CPT-11-induced toxicity was explored.

Methods

Chemicals, antibodies and reagents

β-MCA, ω-MCA, UDCA, HDCA, T-α-MCA, T-β-MCA, T-UDCA, and THDCA were purchased from Steraloids Inc. (Newport, RI). α-MCA, CA, DCA, CDCA, TCDCA, TDCA, and TCA were purchased from Sigma-Aldrich (St Louis, MO). Irinotecan was obtained from Sigma-Aldrich (St Louis, MO). All other reagents and solvents were of HPLC grade. Anti-mouse CD3 (clone 145-2C11), anti-mouse CD28 (clone 37.51), anti-mouse CD16/CD32 (clone 93), anti-mouse CD45 Alexa Fluor® 700 (Clone: 30-F11), anti-mouse CD4 eFluor® 450 (Clone: GK1.5), anti-mouse CD8α PE-Cyanine7 (Clone: 53-6.7), anti-mouse CD8β FITC (Clone: eBioH35-17.2), anti-mouse TCRβ PerCP-Cyanine5.5 (Clone: H57-597), anti-mouse/rat Foxp3 APC (Clone: FJK-16s), anti-mouse IL-10 APC (Clone: JES5-16E3) were from eBiosciences (San Diego, CA). Cytofix/Cytoperm Fixation/Permeabilization Solution and Golgi Plug protein transport inhibitor were purchased from BD Biosciences (Franklin Lakes, NJ). Foxp3 Fix/Perm Buffer Set and mouse IL-10 ELISA kit were purchased from BioLegend (San Diego, CA).

Mouse treatment and samples preparation

Twenty male C57BL/6J (6- to 8-week-old) mice were divided into a vehicle-treated control group (n=10) and a CPT-11-treated group (n=10). All studies involving mice were carried out under protocols approved by the Animal Research Reporting of *In Vivo* Experiments (ARRIVE) guidelines. Mouse handling was performed in accordance with an animal study protocol approved by the National Cancer Institute Animal Care and Use Committee. The mice were maintained under a standard 12 h light/12 h dark cycle with water and chow provided *ad libitum*. CPT-11 was dissolved in dimethyl sulfoxide (DMSO), and then diluted in PBS buffer (v/v=1:1000). CPT-11 (50 mg/kg body weight) was given to mice by a single intraperitoneal injection once per day for eight days. After killing by CO_2 asphyxiation, the gallbladder, liver, duodenum, jejunum, ileum, and colon were harvested, and a small section of each tissue was excised for histological analysis. All the samples were stored at −80°C until analysis. Bile was taken from the gallbladder, and 1 μl of bile diluted with 199 μl of 66% aqueous acetonitrile containing 5 μM chlorpropamide. The homogenates of liver and ileum tissue were prepared and diluted 20 fold with 50% aqueous acetonitrile (5 μM chlorpropamide). All samples were centrifuged at 14,000×g for 20 min, and 5-μl aliquots of the supernatants injected into a Waters UPLC-ESI-QTOFMS system (Waters Corporation, Milford, MA).

Histology analysis

Analysis of liver histology was performed as previously described (Cheng *et al.*, 2014). In brief, small blocks of liver tissues from all mice were immediately fixed in 10% neutral formalin and embedded in paraffin. Sections (4 μm thick) were stained by the hematoxylin

and eosin or Sirius red dyes. Histology of duodenum, jejunum, ileum, and colon tissues was performed as described in a previous study (Kim *et al.*, 2013).

UPLC-ESI-QTOFMS analysis

UPLC-ESI-QTOFMS analysis in full-scan mode at m/z 100–1,000, was performed in the positive and negative modes, as described in a previous study (Li *et al.*, 2013). The liquid chromatography system was an ACQUITY UPLC (Waters Corp., Milford, MA) consisting of a reverse-phase 2.1×50mm ACQUITY UPLC BEH C18 1.7 mm column (Waters Corp.) with a gradient mobile phase consisting of 0.1% formic-acid (solution A) and acetonitrile containing 0.1% formic acid (solution B). The mobile phase composition was maintained at 100% A for 0.5 min, increased to 100% B over the next 7.5 min and returned to 100% A in last 2 min. Nitrogen was used as both cone gas (50 l/h) and desolvation gas (600 l/h). Source and desolvation temperatures were set at 120°C and 350°C, respectively. The capillary and cone voltages were 3000 and 20 V, respectively. Structures of metabolites were elucidated using tandem MS fragmentography with collision energies ranging from 15 to 40 eV.

Data processing and multivariate data analysis (MDA)

MarkerLynx software (Waters Corp.) was used to deconvolute the chromatographic and mass spectrometric data. A multivariate data matrix containing information on sample identity, ion identity (R_t and m/z), and ion abundance was generated through centroiding, deisotoping, filtering, peak recognition, and integration. The data matrix was further analyzed using SIMCA-13.0 software (Umetrics, Kinnelon, NJ). Principle components analysis (PCA) was used to examine the separation of control group and MRS5980-treated group. Potential metabolites were identified by analyzing the ions contributing to the separation of sample groups in the loading scatter plots.

Cell isolation and cell culture

Spleen and mesenteric lymph nodes (MLN) were removed from mice and gently dispersed in DMEM containing 10% FBS to prepare single cell suspensions. The intraepithelial lymphocyte (IEL) and lamina propria lymphocyte (LPL) were isolated from the small intestine by mechanical separation and enzymatic digestion as described (Hall *et al.*, 2008). IL-10 protein in $CD4^+$ T cells was determined by intracellular IL-10 staining by flow cytometry analysis. $CD4^+CD25^-$ T cells to be used for cell culture studies were separated by use of a EasySep™ Mouse $CD4^+CD25^+$ Regulatory T Cell Isolation Kit from Stemcell Technologies, and cultured with plate-bound anti-CD3 (5 μg/ml) and soluble anti-CD28 (2 μg/ml) antibodies in the presence or absence of CPT-11 (20 μg/ml), DCA (20 μg/ml) or TDCA (20 μg/ml) in complete medium for 48 hours. Cells were then collected to determine IL-10 mRNA by quantitative PCR (qPCR), and IL-10 protein measured in culture supernatants by ELISA analysis.

Flow cytometry analysis

The cells were washed using PBS containing 0.5% BSA for 10 min at 300×g, and then incubated with antibodies against CD4, CD8α, CD8β, CD45, TCR-β in staining buffer (PBS containing 0.5% BSA) for 20 minutes, and then fixed with Foxp3 Fix/Perm Buffer Set and

stained with Foxp3, or fixed with Cytofix/Cytoperm Fixation/Permeabilization solution and stained with intracellular IL-10. For intracellular IL-10 staining, the cells were stimulated with PMA, an ionomycin plus protein transport inhibitor (Golgi Plug), for 4 hours in culture medium before staining of the surface markers. Stained cells were analyzed by Fortessa flow cytometry.

Quantitative polymerase chain reaction analysis

Total liver RNA was extracted using TRIzol reagent (Invitrogen, Carlsbad, CA), and cDNA was generated from 1 μg RNA with a SuperScript II^{TM} Reverse Transcriptase kit and random oligonucleotides (Invitrogen, Grand Island, NY). qPCR was performed using SYBR green PCR master mix and ABI Prism 7900HT Sequence Detection System (Applied Biosystems, Foster City, CA). The primer pairs were designed using qPrimerDepot, and messenger RNA quantitation was performed using the comparative cycle threshold (CT) method. The expression of mRNA was normalized to mouse *b β-actin* or *Hprt* mRNA.

Statistical analysis

The experimental data were presented as mean±S.E.M. Comparisons between two groups were performed using a two-tailed unpaired student's t test or Tukey analysis. For all the tests, a value of $P<0.05$ was considered to be statistically significant.

Results

CPT-11 induced phenotype alteration of mice

Treatment with CPT-11 for eight days significantly induced body weight loss ($p<0.001$, Fig. 1A), and altered gallbladder appearance (Fig. 1B). Liver histology appeared normal (Fig. 1C) and there was no elevation in the liver toxicity markers ALT and AST. However, histology analysis revealed that the intestine (including duodenum, jejunum, ileum) and colon had a dramatic remodeling of the mucosa, with different degrees of submucosal edema, submucosal hemorrhage, venous congestion, submucosal leukocyte infiltration, exfoliation of epithelial cells, and inflammatory submucosal leukocyte infiltrates, and shortening of villi (Fig. 1D–G).

CPT-11 treatment resulted in altered of bile acids composition

UPLC-ESI-QTOFMS analysis coupled with multivariate data analysis was employed to profile the metabolomes of liver, ileum and bile. Unsupervised principal components analysis separated the CPT-11-treated group from the control vehicle-treated group (Fig. 2). Through searching metabolomic databases (Madison Metabolomics Consortium Database and METLIN) and comparing with authentic standard standards by column retention times, molecular masses and fragmentation patterns (Supplemental figures 1–4), the major compounds contributing the group separation were identified as bile acid metabolites. CPT-11 treatment induced a decrease in T-α-MCA ($p<0.05$), and an elevation of TDCA ($p<0.001$), CA ($p<0.01$) and DCA ($p<0.01$) in liver (Fig. 3). Levels of many bile acid metabolites were changed in bile by treatment with CPT-11. The bile acid metabolites that were decreased upon CPT-11 administration included T-α-MCA ($p<0.001$), T-β-MCA ($p<0.001$), TUDCA ($p<0.001$), THDCA ($p<0.05$), α-MCA ($p<0.001$), w-MCA ($p<0.01$).

Additionally, taurine was also decreased ($p<0.05$). Compared with the control group, the levels of DCA and TDCA were increased in the CPT-11-treated group ($p<0.001$). Notably, in ileum, CPT-11 treatment induced a reduction of T-α-MCA ($p<0.01$), T-β-MCA ($p<0.05$), and taurine ($p<0.01$). In contrast, an elevation of DCA ($p<0.01$) and TDCA ($p<0.05$) was observed. The mRNAs encoded by genes involved in the metabolism and transport of bile acids were also changed (Figure 4). In liver, CPT-11 treatment significantly decreased the expression of *Oatp1a1*, *Ost*α and *Cyp7b1* mRNAs. in ileum, treatment with CPT-11 resulted in decreased expression of *Mrp2* and *Ibabp* mRNAs.

CPT-11 treatment impacts the intestinal immune tolerance

It is well established that $CD4^+Foxp3^+$ regulatory T cells (Treg cells) and IL-10 producing $CD4^+$ T cells play critical roles in maintaining mucosal immune tolerance (Konkel *et al.*, 2011; Wilson *et al.*, 2011; Li *et al.*, 2014). Furthermore, $TCR\alpha\beta^+CD8\alpha\alpha^+$ unconventional T cells in intraepithelial lymphocyte (IEL) can maintain immune balance (van Wijk *et al.*, 2009; Konkel *et al.*, 2011). This suggests that CPT-11 could alter cell populations influencing immune tolerance in the small intestine and these cells may have a role in CPT-11-induced gut toxicity. To verify this hypothesis, lymphocytes were isolated from the small intestine, Treg cells, IL-10 producing $CD4^+$ T cells, and $TCR\alpha\beta^+CD8\alpha\alpha^+$ unconventional T cells, were examined in small intestine. The IL-10-producing CD4 T cell frequency was significant decreased in the lamina propria lymphocytes (LPL) (Fig. 5A and 5B), while Treg cell frequency was not altered after CPT-11 treatment (Fig. 5C). Moreover, the IL-10 concentrations in the serum was significant decreased after CPT-11 treatment (Fig. 5D), suggesting that IL-10 was systematically effected, although the reduction of IL-10 producing $CD4^+$ T cells occurred in the small intestine, and not in spleen or mesenteric lymph nodes (MLN) (Fig. 5A and 5B). In addition, the $TCR\alpha\beta^+CD8aa^+CD8\beta^-$ unconventional T cell frequency in intraepithelial lymphocytes (IEL) was also significant decreased (Fig. 5E and 5F). Together these data indicated that CPT-11 treatment impacts intestinal immune tolerance by suppressing IL-10-producing $CD4^+$ T cells and decreasing the frequency of $TCR\alpha\beta^+CD8\alpha\alpha^+$ unconventional T cells.

DCA and TDCA aggravate IL-10 reduction caused by CPT-11 in CD4+ T cells

As noted earlier, in mice were treated with CPT-11, the alteration in bile acids mainly occurs mainly in the digestive tract. CPT-11 treatment also reduced IL-10 producing $CD4^+$ T cells in the small intestine, but not in other lymphoid organs (Fig. 5A and 5B). Thus, altered bile acid compositions may contribute to the reduction of IL-10 producing $CD4^+$ T cells and the development of mucositis. To investigate whether the changes of bile acids are involved in IL-10 reduction, taurocholic acid (DCA) and taurodeoxycholic acid (TDCA), the most significantly changed bile acids *in vivo* after CPT-11 treatment were used to test their influence to $CD4^+$ T cells. $CD4^+$ Naive T cells were isolated from splenocytes of mice and cultured under TCR stimulation (anti-CD3 plus anti-CD28) for 48 h, with or without CPT-11, DCA and/or TDCA treatment. After culturing, both *Il-10* mRNA expression and IL-10 protein were reduced in CPT-11-treated cells (Fig. 6A and 6B), and DCA and TDCA treatment suppressed IL-10 production (Fig. 6B). Additionally, CPT-11, together with DCA and TDCA treatment, rapidly reduced IL-10 production (Fig. 6A and 6B). These data

indicate that CPT-11 can reduce IL-10 production in $CD4^+$ T cells, and the bile acid-induced changes may intensify the reduction of IL-10 production.

Discussion

Disruption of the bile acid cycle has been observed in various toxic and disease models. Thus, elucidation of the function of bile acid metabolites in the intestine could facilitate our understanding of the mechanisms associated with toxicity and disease states. For example, lithocholic acid (LCA)-induced hepatotoxicity can disrupt the bile acids homeostasis, and therapeutic targets were found based on the alteration of bile acids, including the TGF-β-SMAD3 signaling pathway (Matsubara *et al.*, 2012) and intestinal cytochrome CYP3A4 (Cheng *et al.*, 2014). The present study demonstrated CPT-11 induced disruption of the bile acids cycle, including altered levels of DCA and TDCA, the most significantly changed bile acids in liver, bile and ileum. This change of bile acid metabolites might be induced by altered expression of genes involved in the metabolism and transport of bile acids. For example, *Oatp1a1*-null mice were found to have increased concentrations of TDCA (Zhang *et al.*, 2012), and the expression of *Oatp1a1* mRNA was decreased in CPT-11-treated mice. Therefore, the role of CPT-11-induced alteration of *Oatp1a1*, *Osta*, and *Cyp7b1* gene expression in liver, and *Mrp2* and *Ibabp* gene expression in ileum in CPT-11-induced intestinal toxicity should be investigated.

Earlier studies focused on the role of immunoregulation in CPT-11-induced intestinal damage (Guabiraba *et al.*, 2014; Lima-Junior *et al.*, 2014). A correlation was noted between the toxicity of CPT-11 and the elevation of pro-inflammation cytokines, but the impact of immune tolerance was not investigated in this study. It is known that the $CD4^+Foxp3^+$ regulatory T cells (Treg cells) and IL-10 producing $CD4^+$ T cells play a critical role in maintaining immune tolerance in the mucosa (Annacker *et al.*, 2003; Konkel *et al.*, 2011; Harrison *et al.*, 2013). $TCR\alpha\beta^+CD8\alpha\alpha^+$ unconventional T cells in intraepithelial lymphocytes can also maintain the immune balance in intestine (Poussier *et al.*, 2002). Therefore, the variation of populations influencing immune tolerance in the small intestine during CPT-11-induced toxicity was investigated, and the results showed that IL-10-producing $CD4^+$ T cells were significantly suppressed. IL-10 is an essential immunoregulator and plays a key role in modulating intestinal inflammation, as mice genetically deficient in IL-10 spontaneously develop severe intestinal inflammation (Rennick *et al.*, 1995; Scheinin *et al.*, 2003). As IL-10 is one of the critical anti-inflammatory cytokines, the present work and previous studies (Lima-Junior *et al.*, 2014) suggest that IL-10 treatment could be a therapeutic approach to alleviate CPT-11-induced mucositis. The correlation between elevation of DCA and TDCA and suppressed production of IL-10 was further investigated using *in vitro* cell experimentation and potentiation of CPT-11-induced decreased IL-10 by these bile acids was demonstrated. In conclusion, the present studies demonstrated that CPT-11-induced metabolic disorders of bile acids cycle potentiate CPT-11-induced suppression of IL-10.

Supplementary Material

Refer to Web version on PubMed Central for supplementary material.

Acknowledgments

This study was funded by the Intramural Research Program of the Center for Cancer Research, National Cancer Institute, National Natural Science Foundation of China (No. 81202586), Tianjin Project of Thousand Youth Talents, and Shandong Natural Science Foundation of China (No. BS2013YY054 and ZR2010HL023).

Abbreviations

CA	cholic acid
CDCA	chenodeoxycholic acid
CPT-11	irinotecan
DCA	deoxycholic acid
HDCA	hydroxyursodeoxycholic acid
IL-10	interleukin-10
MCA	muricholic acid
α-MCA	α-muricholic acid
β-MCA	β-muricholic acid
ω-MCA	ω-muricholic acid
T-α-MCA	tauro-α-muricholic acid
T-β-MCA	tauro-β-muricholic acid
TUDCA	tauro-ursodeoxycholic acid
THDCA	tauro-hydroxyursodeoxycholic acid
T	tauro-chenodeoxycholic acid
TDCA	tauro-deoxycholic acid
TCA	tauro-cholic acid
TCT	T cell receptor
UGT1A1	UDP-glucuronosyltransferase 1A1
UPLC-ESI-QTOFMS	ultra-performance liquid chromatography, electrospray ionization, quadrupole time-of-flight, spectrometry mass spectrometry
UDCA	ursodeoxycholic acid

References

Annacker O, Asseman C, Read S, Powrie F. Interleukin-10 in the regulation of T cell-induced colitis. J Autoimmun. 2003; 20:277–279. [PubMed: 12791312]

Chen S, Yueh MF, Bigo C, Barbier O, Wang K, Karin M, et al. Intestinal glucuronidation protects against chemotherapy-induced toxicity by irinotecan (CPT-11). Proc Natl Acad Sci U S A. 2013; 110:19143–19148. [PubMed: 24191041]

Cheng J, Fang ZZ, Kim JH, Krausz KW, Tanaka N, Chiang JY, et al. Intestinal CYP3A4 protects against lithocholic acid-induced hepatotoxicity in intestine-specific VDR-deficient mice. J Lipid Res. 2014; 55:455–465. [PubMed: 24343899]

Fang ZZ, Krausz KW, Tanaka N, Li F, Qu A, Idle JR, et al. Metabolomics reveals trichloroacetate as a major contributor to trichloroethylene-induced metabolic alterations in mouse urine and serum. Arch Toxicol. 2013; 87:1975–1987. [PubMed: 23575800]

Guabiraba R, Besnard AG, Menezes GB, Secher T, Jabir MS, Amaral SS, et al. IL-33 targeting attenuates intestinal mucositis and enhances effective tumor chemotherapy in mice. Mucosal Immunol. 2014; 7:1079–1093. [PubMed: 24424522]

Hall JA, Bouladoux N, Sun CM, Wohlfert EA, Blank RB, Zhu Q, et al. Commensal DNA limits regulatory T cell conversion and is a natural adjuvant of intestinal immune responses. Immunity. 2008; 29:637–649. [PubMed: 18835196]

Harrison OJ, Powrie FM. Regulatory T cells and immune tolerance in the intestine. Cold Spring Harb Perspect Biol. 2013; 5

Iyer L, King CD, Whitington PF, Green MD, Roy SK, Tephly TR, et al. Genetic predisposition to the metabolism of irinotecan (CPT-11). Role of uridine diphosphate glucuronosyltransferase isoform 1A1 in the glucuronidation of its active metabolite (SN-38) in human liver microsomes. The Journal of clinical investigation. 1998; 101:847–854. [PubMed: 9466980]

Kim JH, Yamaori S, Tanabe T, Johnson CH, Krausz KW, Kato S, et al. Implication of intestinal VDR deficiency in inflammatory bowel disease. Biochim Biophys Acta. 2013; 1830:2118–2128. [PubMed: 23041070]

Konkel JE, Chen W. Balancing acts: the role of TGF-beta in the mucosal immune system. Trends Mol Med. 2011; 17:668–676. [PubMed: 21890412]

Li B, Alli R, Vogel P, Geiger TL. IL-10 modulates DSS-induced colitis through a macrophage-ROS-NO axis. Mucosal Immunol. 2014; 7:869–878. [PubMed: 24301657]

Li F, Jiang C, Krausz KW, Li Y, Albert I, Hao H, et al. Microbiome remodelling leads to inhibition of intestinal farnesoid X receptor signalling and decreased obesity. Nat Commun. 2013; 4:2384. [PubMed: 24064762]

Lima-Junior RC, Freitas HC, Wong DV, Wanderley CW, Nunes LG, Leite LL, et al. Targeted inhibition of IL-18 attenuates irinotecan-induced intestinal mucositis in mice. Br J Pharmacol. 2014; 171:2335–2350. [PubMed: 24428790]

Liu A, Krausz KW, Fang ZZ, Brocker C, Qu A, Gonzalez FJ. Gemfibrozil disrupts lysophosphatidylcholine and bile acid homeostasis via PPARalpha and its relevance to hepatotoxicity. Arch Toxicol. 2014; 88:983–996. [PubMed: 24385052]

Matsubara T, Tanaka N, Sato M, Kang DW, Krausz KW, Flanders KC, et al. TGF-beta-SMAD3 signaling mediates hepatic bile acid and phospholipid metabolism following lithocholic acid-induced liver injury. J Lipid Res. 2012; 53:2698–2707. [PubMed: 23034213]

Nygard SB, Christensen IJ, Nielsen SL, Nielsen HJ, Brunner N, Spindler KL. Assessment of the topoisomerase I gene copy number as a predictive biomarker of objective response to irinotecan in metastatic colorectal cancer. Scand J Gastroenterol. 2014; 49:84–91. [PubMed: 24256029]

Poussier P, Ning T, Banerjee D, Julius M. A unique subset of self-specific intraintestinal T cells maintains gut integrity. J Exp Med. 2002; 195:1491–1497. [PubMed: 12045247]

Rennick D, Davidson N, Berg D. Interleukin-10 gene knock-out mice: a model of chronic inflammation. Clin Immunol Immunopathol. 1995; 76:S174–178. [PubMed: 7554464]

Scheinin T, Butler DM, Salway F, Scallon B, Feldmann M. Validation of the interleukin-10 knockout mouse model of colitis: antitumour necrosis factor-antibodies suppress the progression of colitis. Clin Exp Immunol. 2003; 133:38–43. [PubMed: 12823276]

Umezawa T, Kiba T, Numata K, Saito T, Nakaoka M, Shintani S, et al. Comparisons of the pharmacokinetics and the leukopenia and thrombocytopenia grade after administration of irinotecan and 5-fluorouracil in combination to rats. Anticancer Res. 2000; 20:4235–4242. [PubMed: 11205253]

van Wijk F, Cheroutre H. Intestinal T cells: facing the mucosal immune dilemma with synergy and diversity. Semin Immunol. 2009; 21:130–138. [PubMed: 19386513]

Wilson MS, Ramalingam TR, Rivollier A, Shenderov K, Mentink-Kane MM, Madala SK, et al. Colitis and intestinal inflammation in IL10−/− mice results from IL-13Ralpha2-mediated attenuation of IL-13 activity. Gastroenterology. 2011; 140:254–264. [PubMed: 20951137]

Xue H, Sawyer MB, Field CJ, Dieleman LA, Baracos VE. Nutritional modulation of antitumor efficacy and diarrhea toxicity related to irinotecan chemotherapy in rats bearing the ward colon tumor. Clin Cancer Res. 2007; 13:7146–7154. [PubMed: 18056195]

Zhang Y, Limaye PB, Lehman-McKeeman LD, Klaassen CD. Dysfunction of organic anion transporting polypeptide 1a1 alters intestinal bacteria and bile acid metabolism in mice. PLoS One. 2012; 7:e34522. [PubMed: 22496825]

Highlights

- CPT-11 is an effective anticancer drug, but induced toxicity limits its application in the clinic.
- CPT-11 decreased IL-10-producing CD4 T cell frequency in intestinal lamina propria lymphocytes.
- CPT-11 altered the composition of bile acid metabolites, notably DCA and TDCA in liver, bile and intestine.
- DCA and TDCA potentiated CPT-11-induced suppression of IL-10 secretion by active $CD4^+$ naive T cells.

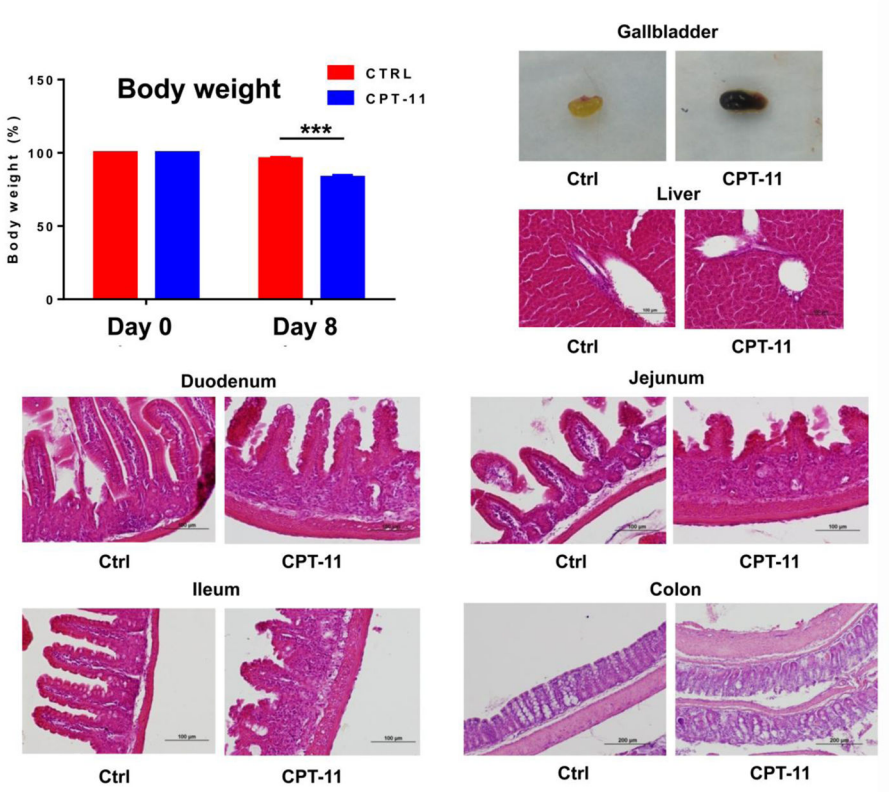

Fig. 1.

Phenotype of mice after intraperitoneal (i.p.) injection of CPT-11 (50 mg/kg). (A) Body weight loss, (B) gallbladder color change, (C) liver histology, (D) duodenum histology, (E) jejunum histology, (F) ileum histology, and (G) colon histology ***, $p<0.001$.

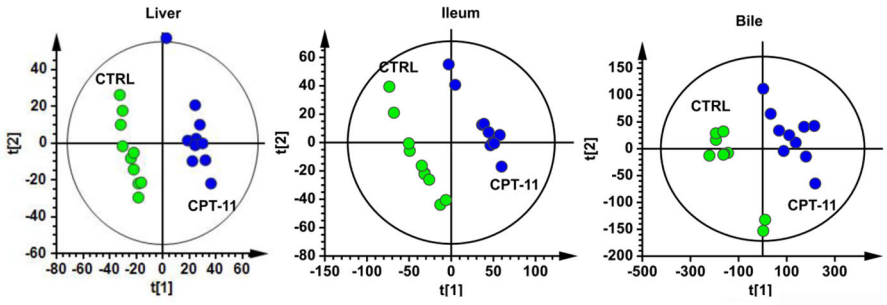

Fig. 2.

PCA scores scatter plots of liver, ileum and bile from the vehicle-treated control group and the CPT-11-treated mice (10 mice/group). The green circles represent the vehicle-treated control group, and the blue represent the CPT-11-treated group.

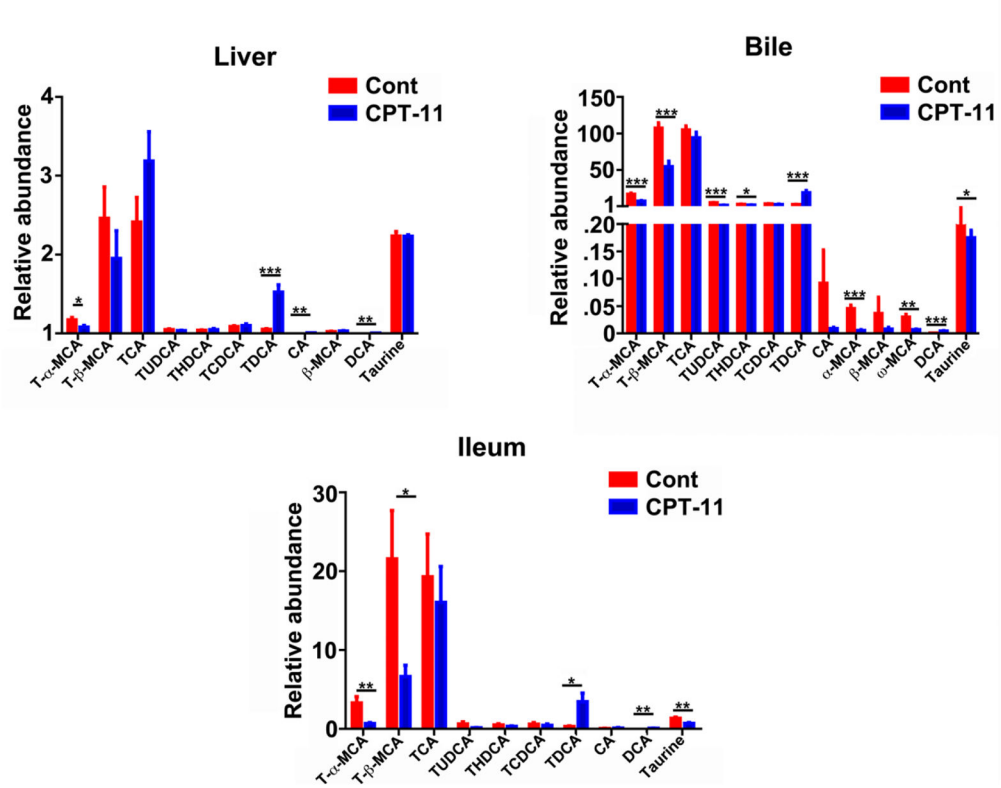

Fig. 3.

Comparisons of the relative abundance of bile acid components between the vehicle-treated control group and the CPT-11-treated group. The red bar represents control group, and the blue bar represents CPT-11-treated group. The value are given as mean plus S.E.M. (n=10). *, $p<0.05$; **, $p<0.01$; ***, $p<0.001$.

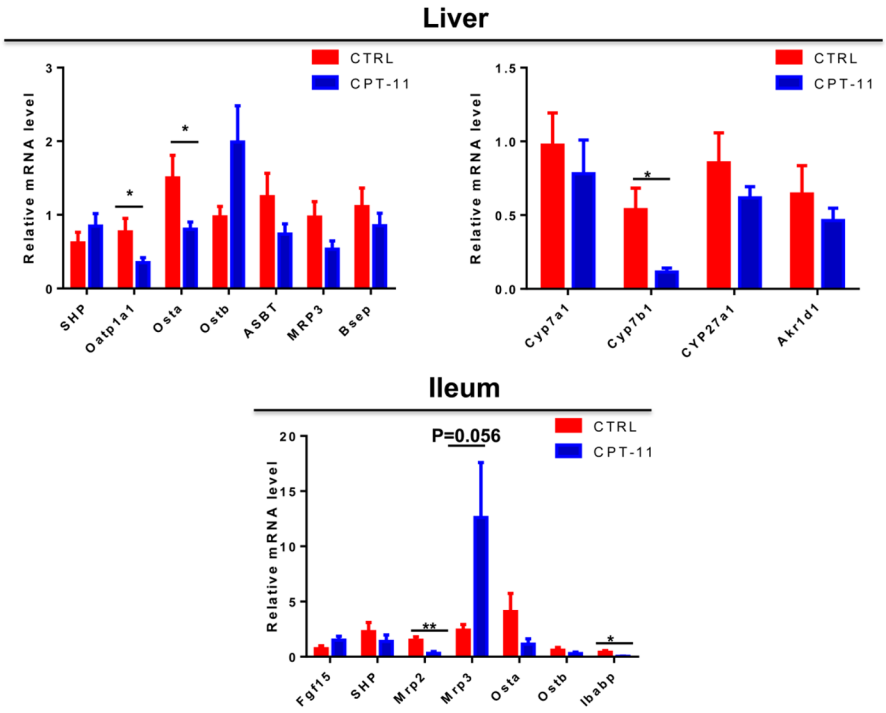

Fig. 4.

The influence of CPT-11 on the expression of mRNAs encoded by genes related involved in the metabolism and transport of bile acids. The value are given as mean plus S.E.M. (n=10).*, $p<0.05$.

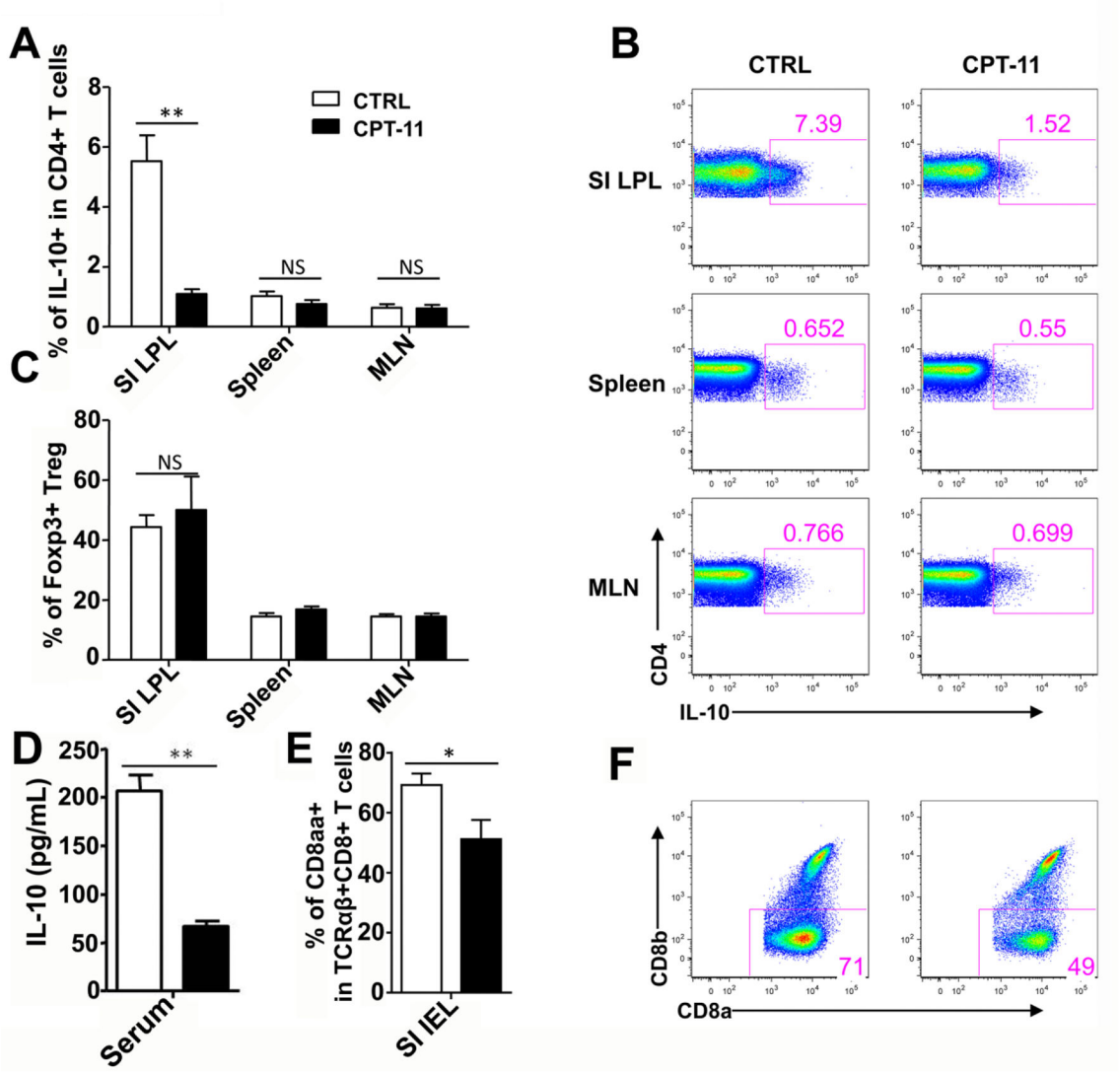

Fig. 5.

CPT-11 treatment affects the intestinal immune tolerance *in vivo*. (A) Bar graph showing the frequency of IL-10$^+$ CD4$^+$ T cells in the small intestine lamina propria lymphocyte (SI LPL, left), spleen (middle) and mesenteric lymph nodes (MLN, right) of the vehicle-treated control and CPT-11-treated mice. (B) Representative FACS plots showing IL-10 staining from TCRαβ$^+$CD4$^+$ T cells isolated from SI LPL (upper), spleen (middle) and MLN (lower) of vehicle-treated control and CPT-11-treated mice. (C) Bar graph showing frequency of Foxp3$^+$ Treg cells in SI LPL (left), spleen (middle) and MLN (right) of the vehicle-treated control and CPT-11-treated mice. (D) Bar graph shows IL-10 concentration in serum of vehicle-treated control and CPT-11-treated mice. (E) Bar graph showing the frequency of TCRαβ+CD8aa+CD8b-unconventional T cells in the small intestine intraepithelial lymphocyte (SI IEL) of the vehicle-treated control and CPT-11-treated mice. (F) Representative FACS plots showing CD8α against CD8β staining from TCRαβ$^+$CD8$^+$ T cells isolated from SI IEL of vehicle-treated control and CPT-11-treated mice. Data shown

are representative of two independent experiments. n=4 (control) or 5 (CPT-11-treated). Unpaired t-test. *p<0.05, **p<0.01.

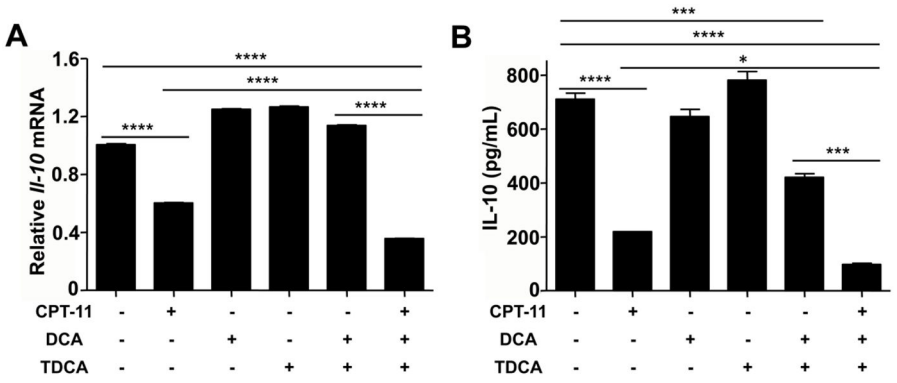

Fig. 6.

DCA and TDCA influence reduction of IL-10 caused by CPT-11 in $CD4^+$ T cells. $CD4^+$ Naive T cells were isolated from mice splenocytes and cultured with anti-CD3 plus anti-CD28 for 48hrs. (A) Bar graph showing *Il-10* mRNA expression in T cells cultured with or without CPT-11, DCA and/or TDCA. Data were presented relative to *Hprt* mRNA expression. (B) Bar graph showing IL-10 production in the culture media of (A). Data shown are representative of three independent experiments. One-way ANOVA followed by Tukey analysis. *$p<0.05$, ***$p<0.001$, ****$p<0.0001$.